J|A|C|S
ARTICLES
Published on Web 01/12/2006

The Chemistry of Dinuclear Analogues of the Anticancer Drug Cisplatin. A DFT/CDM Study†

Dirk V. Deubel*

Contribution from ETH Zurich, USI Campus, Computational Science, D-CHAB, 6900 Lugano, Switzerland

Received September 16, 2005; E-mail: metals-in-medicine@phys.chem.ethz.ch

Abstract: The mechanism of the formation of dinuclear platinum(II) μ-hydroxo complexes from cisplatin hydrolysis products, their interconversion, decomposition, and reactions with biomolecules has been explored using a combined DFT/CDM approach. All activation barriers for the formation of [*cis*-{$Pt(NH_3)_2(X)$}−(μ-OH)−*cis*-{$Pt(NH_3)_2(Y)$}]$^{n+}$ (X, Y = Cl, OH_2, OH) via nucleophilic attack of a hydroxo complex on an aqua complex are lower than the activation barriers for cisplatin hydrolysis. Considering therapeutic Pt(II) concentrations in tumors, however, only the reaction between two molecules of *cis*-$[Pt(NH_3)_2(OH_2)(OH)]^+$ (**E**) yielding [*cis*-{$Pt(NH_3)_2(OH_2)$}−(μ-OH)−*cis*-{$Pt(NH_3)_2(OH)$}]$^{2+}$ (**5**) remains kinetically superior to cisplatin hydrolysis. **5** is strongly stabilized by intramolecular hydrogen bonding between the terminal aqua and hydroxo ligands, resulting in an unusually high pK_a of **5** and a low pK_a of its conjugate acid. Unimolecular cyclization of **5** yields the dimers [*cis*-{$Pt(NH_3)_2$}(μ-OH)]$_2^{2+}$ (**7a** with antiperiplanar OH groups and **7b** with synperiplanar OH groups). The electronic structure of several diplatinum(II) complexes has been analyzed to clarify whether there are metal−metal interactions. The overall reactivity to guanine (Gua) and dimethyl sulfide (Met, representing the thioether functional group of methionine) increases in the order **5** < **7a** ≈ **7b** < mononuclear complexes, whereas the kinetic selectivity to Gua relative to Met increases in the order **7a** ≈ **5** < **7b** ≈ monocationic mononuclear complexes < dicationic mononuclear complex. The results of this work (i) help assess whether dinuclear metabolites play a role in cisplatin chemotherapy, (ii) elucidate the toxicity and pharmacological inactivity of [*cis*-{$Pt(NH_3)_2$}(μ-OH)]$_2^{2+}$, and (iii) suggest future investigations of dinuclear anticancer complexes that contain one μ-hydroxo ligand.

Introduction

Since the discovery of di-μ-hydroxo−bis[*cis*-diammineplatinum(II)],[1] [*cis*-{$Pt(NH_3)_2$}(μ-OH)]$_2^{2+}$, which forms from hydrolysis products of the anticancer drug cisplatin,[2] many diplatinum species and higher oligomers with bridging hydroxo ligands have been characterized.[3] Insights into the mechanism of the formation and decomposition of such dinuclear complexes and their reactions with biomolecules are needed for three reasons: *First*, the potential role of dinuclear cisplatin metabolites in cancer chemotherapy has not been understood entirely. Dinuclear cisplatin derivatives were neither observed in pharmaceutical formulations of cisplatin nor observed in blood substitutes.[4] Lower chloride concentrations than those in pharmaceutical formulations or in extracellular fluids are present inside cells,[5] thus promoting the formation of Pt−OH complexes from cisplatin upon hydrolysis of the Pt−Cl bonds and subsequent deprotonation of the aqua complexes. A hydroxo ligand that attacks as a nucleophile a second platinum complex may be required for the formation of one dinuclear from two mononuclear species. Recent experiments indicated that platinum−μ-hydroxo bonds of diplatinum complexes can be cleaved by guanine-N7.[6] *Second*, [*cis*-{$Pt(NH_3)_2$}(μ-OH)]$_2^{2+}$ was reported to be toxic and pharmacologically inactive[7] when administered intravenously. The toxicity and inactivity could potentially arise from (i) too fast reactions with biomolecules before reaching the target cell, (ii) its fast degradation to reactive

† Quantum chemical studies of metals in medicine, V. Part IV: ref 12.

(1) (a) Lim, M. C.; Martin, R. B. *J. Inorg. Nucl. Chem.* **1976**, *38*, 1911. (b) Faggiani, R.; Lippert, B.; Lock, C. J. L.; Rosenberg, B. *J. Am. Chem. Soc.* **1977**, *99*, 777. (c) Boreham, C. J.; Broomhead, J. A.; Fairlie, D. P. *Aust. J. Chem.* **1981**, *34*, 659. (d) Lippard, S. J. *Science* **1982**, *218*, 1075.

(2) (a) Lippert, B., Ed. *Cisplatin*; Wiley-VCH: Weinheim, 1999. (b) Guo, Z. J.; Sadler, P. J. *Angew. Chem., Int. Ed.* **1999**, *38*, 1512. (c) Fuertes, M. A.; Alonso, C.; Pérez, J. M. *Chem. Rev.* **2003**, *103*, 645. (d) Reedijk, J. *Proc. Natl. Acad. Sci. U.S.A.* **2003**, *100*, 3611. (e) Jakupec, M. A.; Galanski, M.; Keppler, B. K. *Rev. Physiol., Biochem. Pharmacol.* **2003**, *146*, 1. (f) Sigel, A., Sigel, H., Eds. *Metal Ions in Biological Systems*; Marcel Dekker: New York, 2004; Vol. 42. (g) Wang, D.; Lippard, S. J. *Nat. Rev. Drug Discovery* **2005**, *4*, 307.

(3) (a) Faggiani, R.; Lippert, B.; Lock, C. J. L.; Rosenberg, B. *Inorg. Chem.* **1977**, *16*, 1192. (b) Faggiani, R.; Lippert, B.; Lock, C. J. L.; Rosenberg, B. *Inorg. Chem.* **1978**, *17*, 1941. (c) Lippert, B.; Lock, C. J. L.; Rosenberg, B.; Zvagulis, M. *Inorg. Chem.* **1978**, *17*, 2971. (d) Macquet, J.-P.; Cros, S.; Beauchamp, A. L. *J. Inorg. Biochem.* **1985**, *25*, 197. (e) Al-Baker, S.; Vollano, J. F.; Dabrowiak, J. C. *J. Am. Chem. Soc.* **1986**, *108*, 5643. (f) Rochon, F. D.; Morneau, A.; Melanson, R. *Inorg. Chem.* **1988**, *27*, 10. (g) Appleton, T. J.; Mathieson, M.; Byriel, K. A.; Kennard, C. H. L. *Z. Kristallogr.−New Cryst. Struct.* **1998**, *213*, 247. (h) Fekl, U.; van Eldik, R.; Richardson, C.; Robinson, W. T. *Inorg. Chem.* **2001**, *40*, 3247. (i) Yamaguchi, T.; Ito, T. *Adv. Inorg. Chem.* **2001**, *52*, 205. (j) Sakai, K.; Konno, Y.; Takayama, N.; Takahashi, S. *Acta Crystallogr.* **2004**, *B60*, 255. (k) Longato, B.; Bandoli, G.; Dolmella, A. *Eur. J. Inorg. Chem.* **2004**, 1092.

(4) Kristjansson, F.; Sternson, L. A.; Lindenbaum, S. *Int. J. Pharm.* **1988**, *41*, 67.

(5) Alberts, B.; Johnson, A.; Lewis, J.; Raff, M.; Roberts, K.; Walter, P. *Molecular Biology of the Cell*, 4th ed.; Garland: New York, 2002.

(6) Komeda, S.; Lutz, M.; Spek, A. L.; Yamanaka, Y.; Sato, T.; Chikuma, M.; Reedijk, J. *J. Am. Chem. Soc.* **2002**, *124*, 4738.

(7) Gill, D. S.; Rosenberg, B. *J. Am. Chem. Soc.* **1982**, *104*, 4598.

10.1021/ja055741k CCC: $33.50

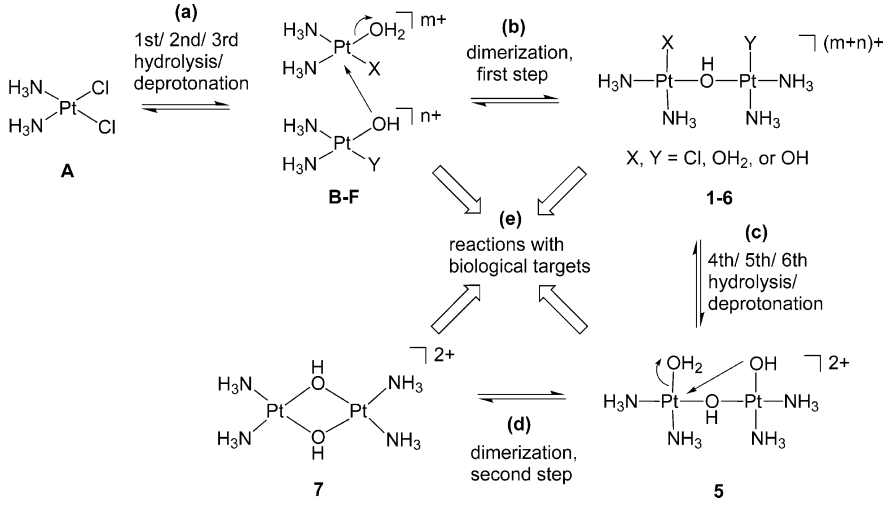

Figure 1. The reactions investigated in this work. See Figures 2 and 3 for the labeling of the Pt−Cl bond hydrolysis reactions.

mononuclear species, (iii) its unfavorable selectivity to purine-N7 positions of DNA, the ultimate target of platinum anticancer drugs, or (iv) the blocking of binding sites of biologically important metal ions by the Pt dication, if it is relatively inert. *Third*, various oligonuclear anticancer complexes[8] including compounds with μ-hydroxo ligands were recently discovered,[9] but relatively little is known about their mode of action. Experimental studies on the reactivity of cisplatin hydrolysis products to biomolecules are complicated by the potential presence of a large number of different compounds and a narrow range of their acidity constants.[10] Modern quantum chemistry could provide information about the activation barriers and reaction free energies of each individual reaction,[11,12] but the reactions of dinuclear species with biomolecules and even the mechanism of their formation have been ignored by theoreticians.[13,14]

The objective of this work is to explore the chemistry of dinuclear cisplatin derivatives with a combined density functional theory (DFT) and continuum dielectric model (CDM) approach, focusing on the reactions shown in Figure 1: (a) Cisplatin (**A**) and other mononuclear *cis*-diammineplatinum(II) species (**B**−**F**) may be transformed into one other via up to three steps of hydrolysis of platinum−chloro bonds (or anation of platinum−aqua bonds) and via deprotonation of aqua complexes (or protonation of hydroxo complexes), as shown in Figure 2. (b) Six different diplatinum complexes (**1**−**6**) that contain one μ-hydroxo ligand may form via the condensation of two mononuclear complexes; we have systematically considered the reactions between all {Pt}−OH species (hydroxo ligand as the best nucleophile) with all {Pt}−OH_2 species (water as the best leaving group). (c) Similar to **A**−**F**, **1**−**6** may be transformed into one other via three additional steps of hydrolysis and

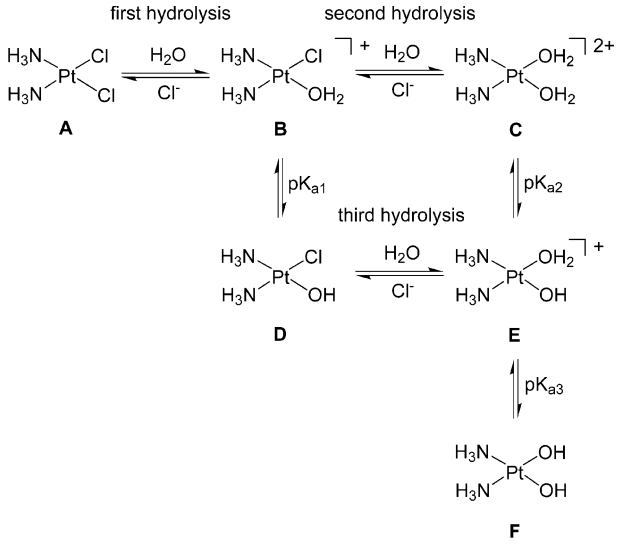

Figure 2. Hydrolysis, anation, and acid−base equilibrium of mononuclear complexes (**A**−**F**). In this work, the hydrolysis of the platinum−chloro bond in *cis*-$[Pt(NH_3)_2(OH)Cl]$ (**D**) is denoted "third hydrolysis".

deprotonation as shown in Figure 3. (d) The cyclization of $[cis\text{-}\{Pt(NH_3)_2(OH_2)\}-(\mu\text{-}OH)-cis\text{-}\{Pt(NH_3)_2(OH)\}]^{2+}$ (**5**) may yield $[cis\text{-}\{Pt(NH_3)_2\}(\mu\text{-}OH)]_2^{2+}$ (**7**), which contains two μ-hydroxo ligands. (e) The platinum aqua complexes may react with biomolecules; their reactions with guanine (Gua) versus dimethyl sulfide (representing methionine, Met) have been compared in the present work. In addition to the comprehensive mechanistic investigation and the prediction of the free energy of all species on a universal scale, emphasis has been placed on exploring the nature of the interaction between the two metal centers in various dinuclear platinum(II) complexes.

Results and Discussion

I. Formation of Dinuclear μ-Hydroxo Pt(II) Complexes. Figure 4a shows the reaction profile calculated at the B3LYP level[15,16] for the formation of mononuclear complexes (**B**−**F**) from cisplatin (**A**) via hydrolysis (blue lines) and deprotonation (orange arrows). All free energies reported in Figure 4 refer to aqueous solution; in addition, selected comparisons with free

(8) Farrell, N. *Met. Ions Biol. Syst.* **2004**, *42*, 251.
(9) Komeda, S.; Lutz, M.; Spek, A. L.; Chikuma, M.; Reedijk, J. *Inorg. Chem.* **2000**, *39*, 4230.
(10) Berners-Price, S. J.; Frenkiel, T. A.; Frey, U.; Ranford, J. D.; Sadler, P. J. *Chem. Commun.* **1992**, 789.
(11) Baik, M. H.; Friesner, R. A.; Lippard, S. J. *J. Am. Chem. Soc.* **2003**, *125*, 14082.
(12) Lau, J. K.-C.; Deubel, D. V. *Chem.-Eur. J.* **2005**, *11*, 2849.
(13) Quantum chemical studies of $[cis\text{-}\{Pt(NH_3)_2\}(\mu\text{-}OH)]_2^{2+}$: (a) Belyaev, A. N.; Panina, N. S.; Simanova, S. A. *Russ. J. Gen. Chem.* **2003**, *73*, 1665. (b) Panina, N. S.; Belyaev, A. N.; Simanova, S. A. *Russ. J. Gen. Chem.* **2003**, *73*, 1835. (c) Panina, N. S.; Beljaev, A. N.; Simanova, S. A.; Calligaris, M. *Int. J. Quantum Chem.* **2004**, *96*, 80.
(14) Deubel, D. V. *Chem. Rev.*, in preparation.
(15) Becke, A. D. *J. Chem. Phys.* **1993**, *98*, 5648.
(16) Lee, C. T.; Yang, W. T.; Parr, R. G. *Phys. Rev. B* **1988**, *37*, 785.

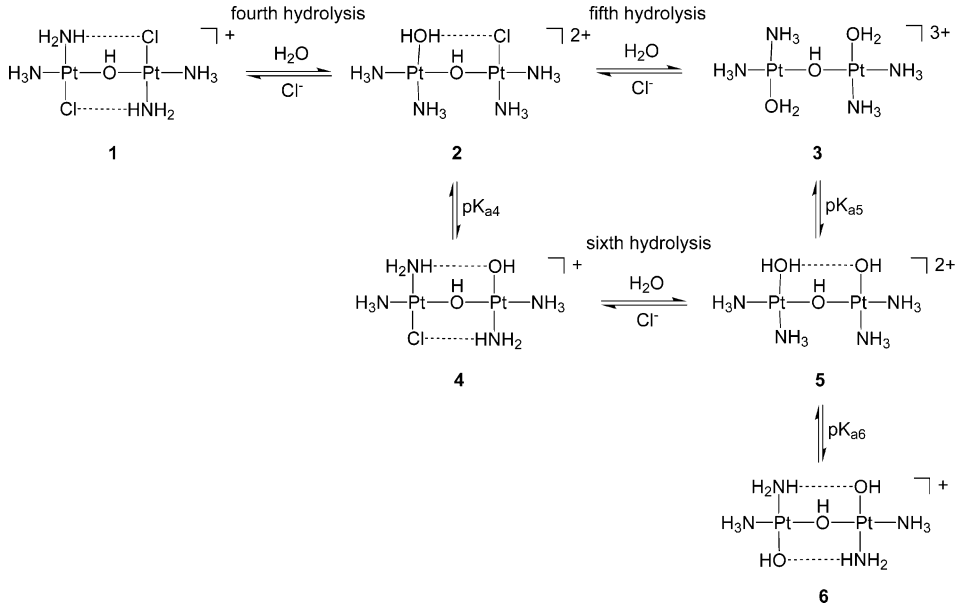

Figure 3. Hydrolysis, anation, and acid−base equilibrium of dinuclear complexes (**1**−**6**). Dashed lines indicate hydrogen bonding found in the most stable isomer. For calculated structures, see the Supporting Information.

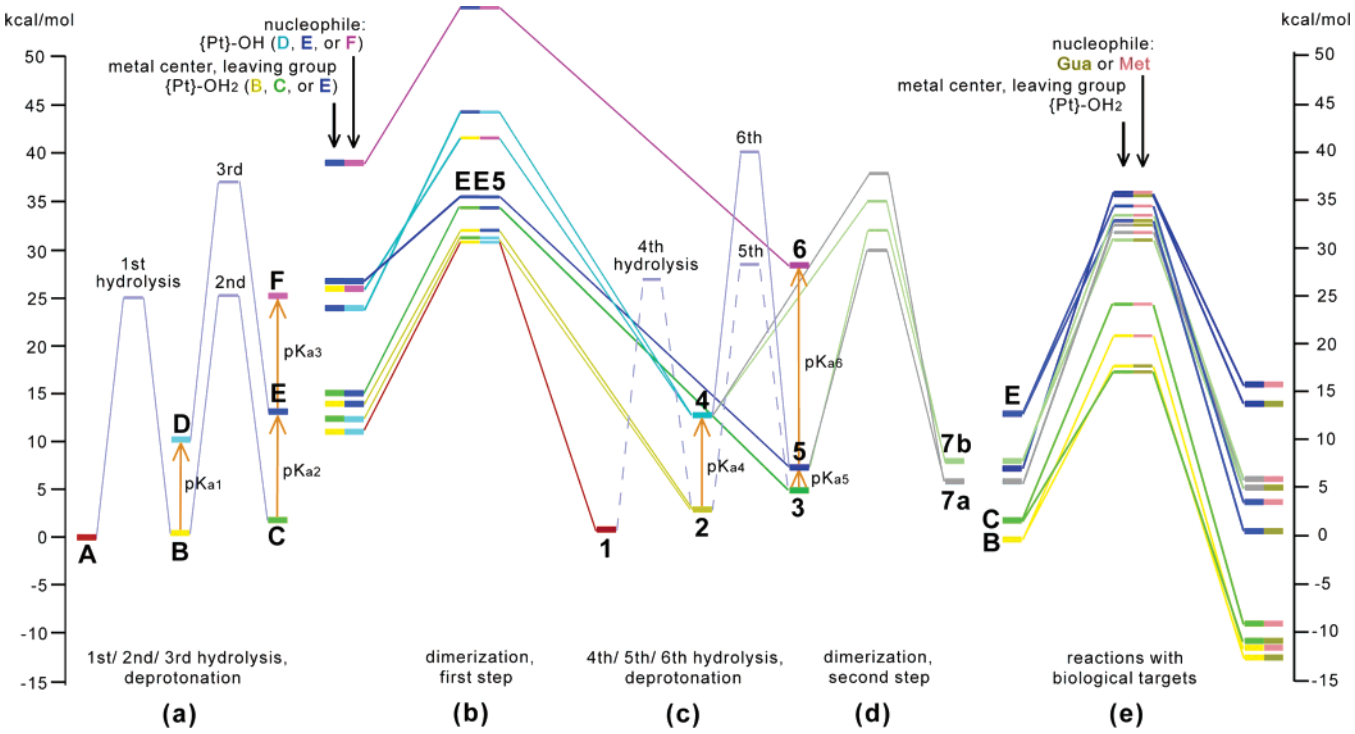

Figure 4. Simplified reaction profile on a universal free energy scale. Thick bars represent molecules, and thin bars represent transition states. (a) Hydrolysis, anation, and acid−base equilibrium of mononuclear complexes (**A**−**F**). (b) Formation of dinuclear complexes (**1**−**6**) containing one μ-hydroxo ligand upon nucleophilic attack of a {Pt}−OH group at the metal center of a {Pt}−OH_2 complex. All free energies of the reactants are given relative to two cisplatin molecules. (c) Hydrolysis, anation, and acid−base equilibrium of dinuclear complexes (**1**−**6**). Dashed lines indicate estimated barriers. (d) Formation of dinuclear complexes (**7a** and **7b**) containing two μ-hydroxo ligands from **4** and **5**. (e) Reaction of **B**, **C**, **E**, **5**, **7a**, and **7b** with guanine (Gua) and dimethyl sulfide (Met); the activation barriers are also listed in Table 1. Separated parts a−e of this figure are provided in the Supporting Information.

energies in vacuo will be made in the text. Tabulated values of the free energies in Figure 4 are given in the Supporting Information. It is important to note that we predict similar activation barriers (∼25−27 kcal/mol) and similar reaction free energies (∼0−2 kcal/mol) for all three hydrolysis reactions, in contrast to some of the former studies that used reactant adducts and product adducts rather than the separated reactants and products as a reference state.[17,18] Technical details and pitfalls in the interpretation of quantum chemical calculations of cisplatin hydrolysis are discussed elsewhere.[19] As shown in Table S-1, experimental activation and reaction free energies of Pt−Cl and Ru−Cl bond hydrolysis and the pK_a values of the aqua complexes[20] are reproduced with a remarkable absolute accuracy of approximately 4 kcal/mol; the relative accuracy (when similar reactions are compared to each other) is significantly better. Fully consistent with the pK_a values, the hydroxo complexes (**D**, **E**, **F**) are higher in free energy (by $RT \ln 10 \times$ pK_a) than their conjugated acids (**B**, **C**, **E**). Nevertheless, the

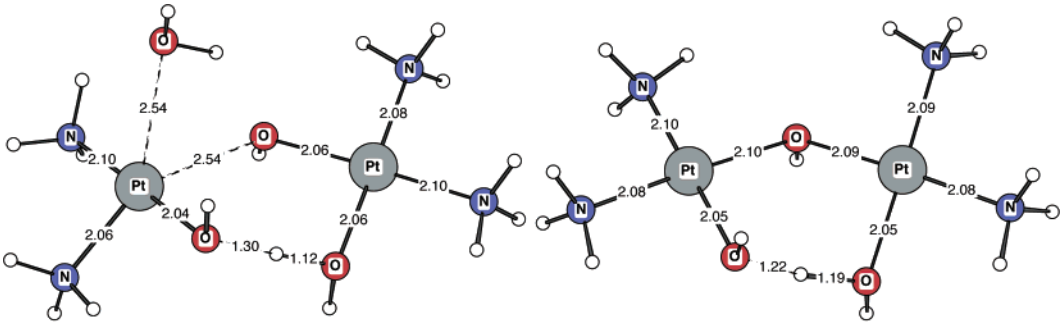

Figure 5. Calculated structure of TS **EE5** and [*cis*-{Pt(NH$_3$)$_2$(OH$_2$)}−(μ-OH)−*cis*-{Pt(NH$_3$)$_2$(OH)}]$^{2+}$ (**5**). All distances are in angstroms.

hydroxo complexes remain accessible at physiological pH and temperature because of the low concentration of hydronium ion relative to that of water. The exact speciation in vivo depends on the local pH in the vicinity of macromolecules[21] and on the effect of macromolecules on hydrolysis rates.[22]

Figure 4b displays the predicted reaction profile for the formation of the dinuclear complexes **1**−**6** via nucleophilic attack of the hydroxo ligand of **D**, **E**, or **F** on the metal center of **B**, **C**, or **E**, which contain an aqua ligand as the leaving group.[23] A systematic investigation of all reactions leading to **1**−**6** reveals that typical activation free energies (∼20 kcal/mol) are significantly lower than those for the hydrolysis of the mononuclear (Figure 4a) and dinuclear complexes (Figure 4c). Given a typical platinum peak concentration of 15−40 μM in tumors[24] after intravenous or intra-arterial perfusion, which is some 6 orders of magnitude smaller than the concentration of water in water, the formation of diplatinum compounds may be competitive to cisplatin hydrolysis if the activation barrier is lower than that of hydrolysis minus 6 × *RT* ln 10 (i.e., lower than ∼17−19 kcal/mol). While most barriers for the formation of **1**−**6** from **B**−**F** are not below this threshold, there is one exception (Figure 4b): The transition state (TS) **EE5** is calculated to be only 9 kcal/mol higher in free energy than the reactants, two molecules of **E**.

Inspection of the structure of TS **EE5** (Figure 5) indicates a strong hydrogen bond similar to that reported in the TS for the reaction of *cis*-[Pt(NH$_3$)$_2$(OH$_2$)$_2$]$^{2+}$ (**C**) with guanine.[11] The calculated free energy profile in Figure 4 shows that the product [*cis*-{Pt(NH$_3$)$_2$(OH$_2$)}−(μ-OH)−*cis*-{Pt(NH$_3$)$_2$(OH)}]$^{2+}$ (**5**, Figure 5) is like TS **EE5** stable as well. The calculated structures demonstrate that the bent Pt−(μ-OH)−Pt moiety in [*cis*-{Pt(NH$_3$)$_2$(X)}−(μ-OH)−*cis*-{Pt(NH$_3$)$_2$(Y)}]$^{n+}$ (**1**−**6**) complexes may enforce the interaction of X and Y either with each other or with the ammine ligands. As is schematically shown in Figure 3, the monocationic complexes **1**, **4**, and **6** have two intramolecular hydrogen bonds and a remarkably short Pt−Pt distance (3.17 Å in **6**), while the dicationic species **2** and **5** have one and the tricationic species **3** has no intramolecular hydrogen bond (for structural drawings, see the Supporting Information). In **5**, the strongest hydrogen bond donor (aqua ligand) meets the strongest hydrogen bond acceptor (hydroxo ligand). The stability of **5** is reflected by the predicted pK_a values (Figure 4c, orange arrows): The pK_a of **3** is low (2.0) and the pK_a is of **5** is high (15.5), in comparison with the pK_a of **2** (6.7) and those of the mononuclear complexes (vide supra). There is a recent experimental example of a similar lowering of acidity constants by inter-ligand communication in a mononuclear Pt complex: *trans*-diamminebis(1,9-dimethyladeninium)platinum(II).[25]

Figure 4d displays the calculated reaction profile for the cyclization of **5**, the final step in the formation of [*cis*-{Pt(NH$_3$)$_2$}(μ-OH)]$_2^{2+}$. The terminal hydroxo ligand of **5** attacks in a nucleophilic manner at the adjacent metal center, where the terminal aqua ligand is displaced. The corresponding reaction of **4** with chloride instead of water being the leaving group (also displayed in Figure 4d) would have been a viable alternative, if the formation of **4** from mononuclear species or from **1**−**6** had been as easy as is the formation of **5** from **E**.[26] Although the activation free energies (23−26 kcal/mol) for the final step are higher than those for the reactions between the mononuclear cisplatin hydrolysis products, the cyclization is unimolecular and thus likely not rate-determining. This result is consistent with a kinetic study on the formation of di-μ-hydroxo-bis[(*trans*-1,2-diaminocyclohexane)platinum(II)].[7] The calculations show that there are two stable isomers of the dimer, [*cis*-{Pt(NH$_3$)$_2$}-

(17) Quantum chemical studies of cisplatin hydrolysis: (a) Burda, J. V.; Zeizinger, M.; Sponer, J.; Leszczynski, J. *J. Chem. Phys.* **2000**, *113*, 2224. (b) Chval, Z.; Sip, M. *J. Mol. Struct. (THEOCHEM)* **2000**, *532*, 59. (c) Zhang, Y.; Guo, Z. J.; You, X. Z. *J. Am. Chem. Soc.* **2001**, *123*, 9378. (d) Zeizinger, M.; Burda, J. V.; Sponer, J.; Kapsa, V.; Leszczynski, J. *J. Phys. Chem. A* **2001**, *105*, 8086. (e) Cooper, J.; Ziegler, T. *Inorg. Chem.* **2002**, *41*, 6614. (f) Raber, J.; Llano, J.; Eriksson, L. A. In *Quantum Medicinal Chemistry*; Carloni, P., Alber, F., Eds.; Wiley-VCH: Weinheim, 2003; p 113. (g) Robertazzi, A.; Platts, J. A. *J. Comput. Chem.* **2004**, *25*, 1060. (h) Burda, J. V.; Zeizinger, M.; Leszczynski, J. *J. Chem. Phys.* **2004**, *120*, 1253. (i) Raber, J.; Zhu, C.; Eriksson, L. A. *Mol. Phys.* **2004**, *102*, 2537. (j) Burda, J. V.; Zeizinger, M.; Leszczynski, J. *Comput. Chem.* **2005**, *26*, 907.

(18) CPMD study: Carloni, P.; Sprik, M.; Andreoni, W. *J. Phys. Chem. B* **2000**, *104*, 823.

(19) Lau, J. K.-C.; Deubel, D. V. *J. Chem. Theory Comput.* **2006**, *2*, 103−106.

(20) pK_a calculated: **B** (7.8), **C** (8.3), and **E** (9.5). Exp (ref 10): **B** (6.41), **C** (5.37), and **E** (7.21).

(21) Lamm, G.; Pack, G. R. *Proc. Natl. Acad. Sci. U.S.A.* **1990**, *87*, 9033.

(22) Vinje, J.; Sletten, E.; Kozelka, J. *Chem.-Eur. J.* **2005**, *11*, 3863.

(23) The activation barriers for the dimerization reactions of **A**−**F** with chloride as the leaving group were found to be substantially higher (not shown in Figure 4b).

(24) For examples, see: (a) Sileni, V. C.; Fosser, V.; Maggian, P.; Padula, E.; Beltrame, M.; Nicolini, M.; Arslan, P. *Cancer Chemother. Pharmacol.* **1992**, *30*, 221. (b) Kanamori, Y.; Kigawa, J.; Minagawa, Y.; Irie, T.; Itamochi, H.; Cheng, X. S.; Okada, M.; Terakawa, N. *Gynecol. Obstet. Invest.* **1997**, *44*, 57. (c) Alberts, D. S.; Hallum, A. V., III; Stratton-Custis, M.; Garcia, D. J.; Gleason-Guzman, M.; Salmon, S. E.; Santabarbara, P.; Niesor, E. J.; Floret, S.; Bentzen, C. L. *Clin. Cancer Res.* **2001**, *7*, 1246 (in vitro study). (d) Tegeder, I.; Bräutigam, L.; Seegel, M.; Al-Dam, A.; Turowski, B.; Geisslinger, G.; Kovacs, A. F. *Clin. Pharmacol. Ther.* **2003**, *73*, 417.

(25) (a) Roitzsch, M.; Lippert, B. *J. Am. Chem. Soc.* **2004**, *126*, 2421. (b) Lippert, B. In *Progress in Inorganic Chemistry*; Karlin, K. D., Ed.; Wiley: New York, 2005; Vol. 54, p 385.

(26) Note that here the reactions with chloride as a leaving group (**4** → **7a** or **7b**) are competitive with the reaction with water as a leaving group (**5** → **7a** or **7b**), because **5** is stabilized by a hydrogen bond involving the aqua ligand.

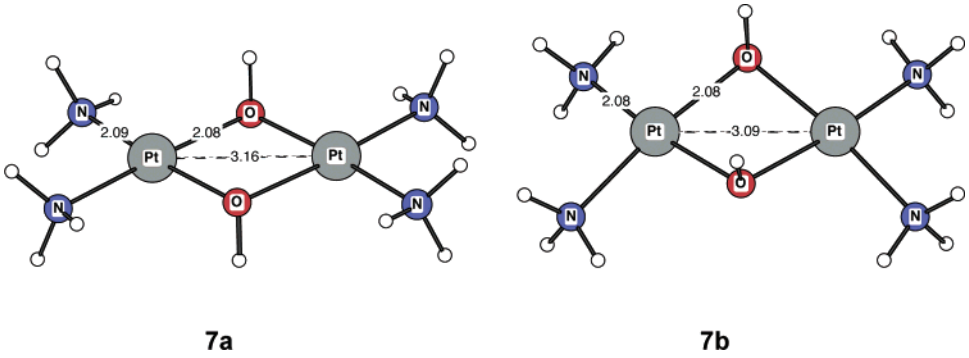

7a **7b**

Figure 6. Calculated structure of $[cis\text{-}\{Pt(NH_3)_2\}(\mu\text{-}OH)]_2^{2+}$ (**7a** and **7b**).

$(\mu\text{-}OH)]_2^{2+}$, as shown in Figure 6. The C_{2h}-symmetric propeller-shaped isomer **7a** (planar Pt_2O_2 core, OH ligands antiperiplanar) is predicted to be 3 kcal/mol less stable in vacuo but −2 kcal/mol more stable in solution (Figure 4d) than the C_{2v}-symmetric butterfly-shaped isomer **7b** (folded Pt_2O_2 core, OH ligands synperiplanar). The similar free energies of **7a** and **7b** indicate that the preference for either isomer in the solid state may depend on the counterion, which is consistent with the report of two X-ray structures with a planar Pt_2O_2 core (nitrate[1b] and carbonate[3c] counterion) and another with a folded Pt_2O_2 core (perchlorate counterion).[3j]

II. Metal−Metal Interactions in Dinuclear Pt(II) Complexes. Both **7a** and **7b** show a remarkably short Pt−Pt distance of 3.16 and 3.09 Å, respectively.[27] The question whether such short distances in covalently and noncovalently linked platinum oligomers imply weak metal−metal "interactions" or "bonds" has been discussed for decades.[28,29] For instance, the strength of metal−metal bonds in various dinuclear d^8 complexes was estimated on the basis of the energies of conformers, in some of which the four-membered $\{M_2X_2\}$ core is folded rather than planar.[29] However, our investigation will cast doubt on the assumption that the folded geometry of these conformers is attributed to metal−metal bonds. A bond between two atoms is unambiguously reflected by the presence of a bond critical point (BCP) in a topological analysis of electron density (ρ).[30] A BCP is a (3,−1) stationary point of ρ that is characterized by a minimum of electron density in the direction of the bond and a maximum of ρ in the two perpendicular directions. Figure 7 displays a contour line diagram of ρ of molecule **7a**. The analysis reveals that there is a stationary point exactly between the two Pt atoms, but diagonalization of the Hessian of ρ showed that it is a ring critical point (RCP) rather than a BCP, indicating that the two metal centers do not interact directly with each other. It is important to note that **7b** (not displayed in Figure 7) shows the same electronic structure of electron density at the $\{Pt_2O_2\}$ core as does **7a**: There is also an RCP rather than a BCP between the two metal centers, implying that the folded geometry of the $\{Pt_2O_2\}$ ring arises from conformational preferences of the metals and bridging ligands rather than from metal−metal bonding.

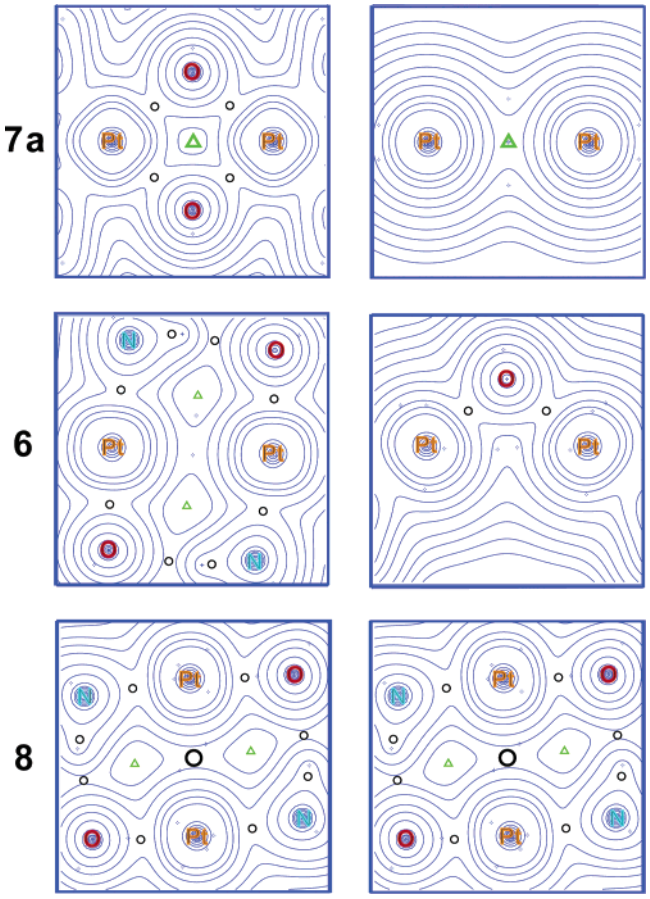

Figure 7. Contour-line plot of electron density in **7a**, **6**, and **8** in two perpendicular planes that both contain both platinum atoms. Black open circles are bond critical points (BCP), and green triangles are ring critical points (RCP). Big symbols are critical points between the two metal centers.

We have analyzed two other dinuclear platinum(II) complexes that have a short Pt−Pt distance as well. First, $[cis\text{-}\{Pt(NH_3)_2(OH)\}\text{-}(\mu\text{-}OH)\text{-}cis\text{-}\{Pt(NH_3)_2(OH)\}]^+$ (**6**, structure in Figure 8) is among **1**−**6** the complex with the shortest Pt−Pt distance (3.17 Å). The analysis shows that there is no stationary point at all between the two metal centers. Second, the dimer $cis\text{-}[Pt(NH_3)_2(OH)_2]_2$ (**8**, structure also in Figure 8) consists of two monomer units $cis\text{-}[Pt(NH_3)_2(OH)_2]$ (**F**) and is an analogue of Magnus salt, $Pt(NH_3)_4PtCl_4$.[28] Such platinum piles with Pt in a d^8 or partially oxidized ($\sim d^{7.7}$) configuration are of current interest.[31] The Pt−Pt distance in **8** is as short as that in **7b** (3.09 Å). In contrast to the other dinuclear complexes, there is a BCP between the two metals in **8**. However, the value of electron density ρ at this BCP in **8** (0.030 atomic units, au)

(27) Experimental Pt−Pt distance (crystal structures): 3.085 and 3.104 Å (**7a**), 3.042 Å (**7b**).
(28) Atoji, M.; Richardson, J. W.; Rundle, R. E. *J. Am. Chem. Soc.* **1957**, *79*, 3017.
(29) Aullón, G.; Ujaque, G.; Lledós, A.; Alvarez, S. *Chem.-Eur. J.* **1999**, *5*, 1391.
(30) (a) Bader, R. F. W. *Chem. Rev.* **1991**, *91*, 893. (b) Bader, R. F. W. *Atoms in Molecules. A Quantum Theory*; Oxford University Press: Oxford, U.K., 1994.

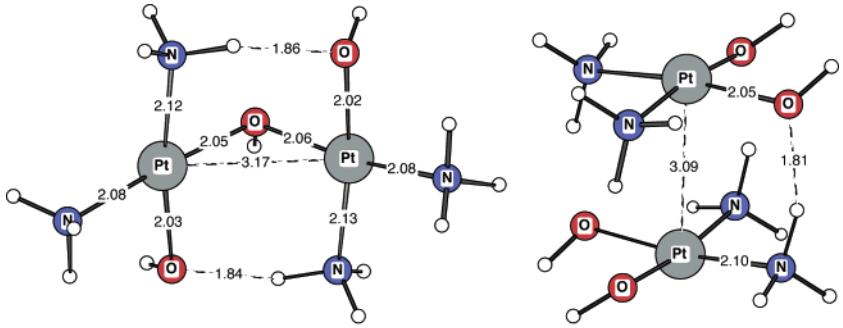

6 **8**

Figure 8. Calculated structure of [*cis*-{Pt(NH$_3$)$_2$(OH)}−(μ-OH)−*cis*-{Pt(NH$_3$)$_2$(OH)}]$^+$ (**6**) and [*cis*-Pt(NH$_3$)$_2$(OH)$_2$]$_2$ (**8**).

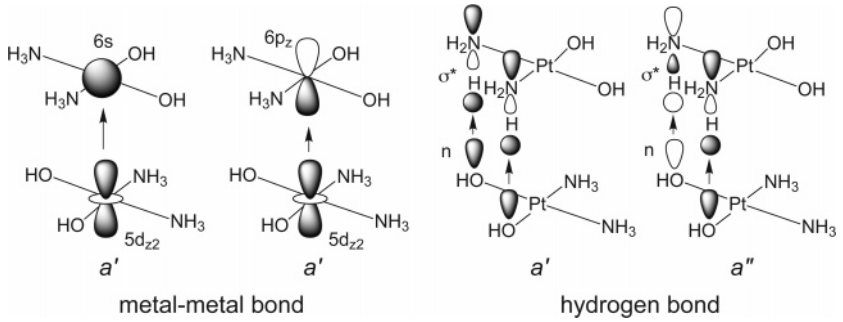

Figure 9. Selected a′ and a″-symmetric donor and acceptor orbitals in [*cis*-Pt(NH$_3$)$_2$(OH)$_2$]$_2$ (**8**).

is only slightly greater than that at the RCP in **7a** (0.028 au) and as small as that at the RCP in **7b** (0.030 au).

To characterize the metal−metal interaction in **8** further, we have analyzed the molecule in terms of interactions between the two monomers *cis*-[Pt(NH$_3$)$_2$(OH)$_2$] (**F**) using an energy decomposition scheme[32] at the BP86 level with large basis sets. Because a clear identification of such weak interactions in the molecular orbitals of **8** has been difficult, the analysis has been performed in C_s symmetry to reveal the energy contributions from a′ and a″ symmetry orbitals to the stabilizing orbital interactions. The idea behind this orbital-symmetry consideration is the fact that a σ bond between the metals in **8** can only have a′ symmetry, whereas intermolecular hydrogen bonding between the ammine and hydroxo ligands shall have contributions from both symmetric (a′) and anti-symmetric combinations (a″) of molecular orbitals (Figure 9). The analysis reveals that the energy contribution from a′ (−28 kcal/mol) is not much stronger than that from a″ (−21 kcal/mol), indicating that intramolecular hydrogen bonding in **8** is much more important than the electron donation from occupied metal 5d$_{z^2}$ orbitals into vacant 6s and 6p$_z$ orbitals. If binding metal−metal interactions had been predominant in **8**, the a′ contribution would have been much stronger than that of a″. Moreover, the overall contribution (a′ + a″) from the stabilizing orbital interactions (−49 kcal/mol) to the total bonding energy is found to be only one-half of the electrostatic stabilization (−97 kcal/mol) between the two monomer units **F** in the dimer **8**. These stabilizing interactions are partially compensated by Pauli repulsion (102 kcal/mol) and by the energy required for the deformation of the free monomers **F** toward their structure in the dimer **8** (12 kcal/mol). Overall, **8** is predicted to be −32 kcal/mol (−49 − 97 + 102 + 12) more stable in vacuo than two molecules of **F**, but 2 kcal/mol less stable at B3LYP in solution than two molecules of **F**.[33]

The location of BCPs has been used to characterize ring strain in cyclic compounds.[30] The carbon−carbon BCPs in highly strained hydrocarbons such as cyclobutane are clearly outside the polygon, whereas the BCPs in nonstrained hydrocarbons such as cyclohexane are on the edges of the polygon (Figure 10). In contrast, we find that the Pt−O BCPs in **7a** and **7b** are inside the Pt$_2$O$_2$ ring (Figure 10). We have also investigated the platinum-hydroxo analogue of cyclohexane: the trimer [*cis*-{Pt(NH$_3$)$_2$}(μ-OH)]$_3^{3+}$. Two conformers have been found (for structures, see the Supporting Information), with the C_s-symmetric boat-shaped molecule **9a** being −2 kcal/mol more stable both in vacuo and in aqueous solution than the C_{3v}-symmetric crown-shaped isomer **9b**, of which an X-ray structure was reported by the pioneers of this chemistry.[3b] It is interesting to compare the relative free energies of the dimer and trimer using a group-equivalent scheme.[34] Cyclohexane is −29 kcal/mol more stable than the highly strained cyclobutane in vacuo. In contrast, the trimer [*cis*-{Pt(NH$_3$)$_2$}(μ-OH)]$_3^{3+}$ (**9a**) is 2 kcal/mol less stable than the dimer [*cis*-{Pt(NH$_3$)$_2$}(μ-OH)]$_2^{2+}$ (**7a**) in solution. The entire absence of ring strain in **7a** and **7b** illustrates the remarkable stability of the dimers in solution relative to the other species. At sufficiently large platinum concentrations, low chloride concentrations, and appropriate pH,

(31) Examples: (a) Sakai, K.; Takeshita, M.; Tanaka, Y.; Ue, T.; Yanagisawa, M.; Kosaka, M.; Tsubomura, T.; Ato, M.; Nakano, T. *J. Am. Chem. Soc.* **1998**, *120*, 11353. (b) Matsumoto, K.; Sakai, K. *Adv. Inorg. Chem.* **2000**, *49*, 375. (c) Colombi Ciacchi, L.; Pompe, W.; De Vita, A. *J. Am. Chem. Soc.* **2001**, *123*, 7371. (d) Sakai, K.; Ishigami, E.; Konno, Y.; Kajiwara, T.; Ito, T. *J. Am. Chem. Soc.* **2002**, *124*, 12088.

(32) (a) Ziegler, T.; Rauk, A. *Theor. Chim. Acta* **1977**, *46*, 1. (b) Bickelhaupt, F. M.; Baerends, E. J. *Rev. Comput. Chem.* **2000**, *15*, 1. (c) Frenking, G.; Fröhlich, N. *Chem. Rev.* **2000**, *100*, 717. (d) Frenking, G.; Wichmann, K.; Fröhlich, N.; Loschen, C.; Lein, M.; Frunzke, J.; Rayón, V. M. *Coord. Chem. Rev.* **2003**, *238*, 55.

(33) Dimerization energy in vacuo: −32 kcal/mol (BP86, energy decomposition scheme), −26 kcal/mol (B3LYP). Dimerization free energy in solution: +2 kcal/mol (B3LYP).

(34) $^3/_2$[*cis*-{Pt(NH$_3$)$_2$}(μ-OH)]$_2^{2+}$ → [*cis*-{Pt(NH$_3$)$_2$}(μ-OH)]$_3^{3+}$. Cf.: Bach, R. D.; Dmitrenko, O. *J. Am. Chem. Soc.* **2004**, *126*, 4444.

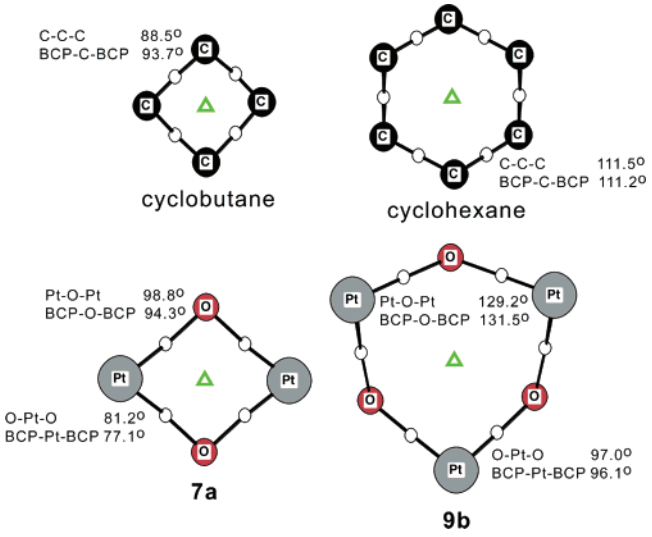

Figure 10. Bond critical points (BCP, black circles) corresponding to C−C and Pt−O bonds and ring critical points (RCP, green triangles) in (a) cyclobutane, (b) cyclohexane, chair conformation, (c) [*cis*-{Pt(NH$_3$)$_2$}(μ-OH)]$_2^{2+}$ (**7a**), and (d) [*cis*-{Pt(NH$_3$)$_2$}(μ-OH)]$_3^{3+}$ (**9b**).

Table 1. Calculated Activation Free Energies (in kcal/mol) for the Reaction of **B**, **C**, **E**, **5**, **7a**, and **7b** with Gua and Met

metal complex	Gua	Met	average	difference[a]
cis-[Pt(NH$_3$)$_2$(OH$_2$)Cl]$^+$ (**B**)	17.9	20.9	19.4	−3.0
cis-[Pt(NH$_3$)$_2$(OH$_2$)$_2$]$^{2+}$ (**C**)	15.6	22.8	19.2	−7.2
cis-[Pt(NH$_3$)$_2$(OH$_2$)(OH)]$^+$ (**E**)	19.5	21.3	20.4	−1.8
[*cis*-Pt(NH$_3$)$_2$(OH$_2$)−(μ-OH)−*cis*-Pt(NH$_3$)$_2$(OH)]$^{2+}$ (**5**)	27.8	27.8	27.8	0.0
[*cis*-{Pt(NH$_3$)$_2$}(μ-OH)]$_2^{2+}$ (**7a**)	26.4	25.4	25.9	+1.0
[*cis*-{Pt(NH$_3$)$_2$}(μ-OH)]$_2^{2+}$ (**7b**)	23.0	25.4	24.2	−2.4

[a] Gua relative to Met platination. The more negative are the values, the more selectively binds the metal complex to Gua.

the dimers are the predominant species, and the knowledge of their reactivity to biomolecules is crucial.

III. Reactions of Pt(II) Complexes with Biomolecules. Figure 4e displays the calculated activation and reaction free energies for the reaction of **5**, **7a**, **7b**, *cis*-[Pt(NH$_3$)$_2$(OH$_2$)Cl]$^+$ (**B**), *cis*-[Pt(NH$_3$)$_2$(OH$_2$)$_2$]$^{2+}$ (**C**), and *cis*-[Pt(NH$_3$)$_2$(OH$_2$)(OH)]$^+$ (**E**) with guanine ("Gua") and dimethyl sulfide ("Met", representing the thioether functional group in methionine). Because of the kinetic control of the platination of biomolecules,[2d] we discuss only activation free energies, which are also listed in Table 1. Note that the platination of thiols (representing cysteine residues, Cys, e.g., in glutathione, GSH) has barriers similar to the platination of Met, whereas thiolates likely react as thiols and are deprotonated after metal binding.[12] The reactions of the mononuclear complexes **B** and **C** in solution were investigated recently using DFT/CDM methods.[11,35] We now find that the activation and reaction free energies for the reactions of *cis*-[Pt(NH$_3$)$_2$(OH$_2$)(OH)]$^+$ (**E**) are similar to those of *cis*-[Pt(NH$_3$)$_2$(OH$_2$)Cl]$^+$ (**B**).[36] It is important to distinguish reactivity and selectivity: The overall reactivity may be characterized by the average of the barriers for Gua and Met platination, selectivity by the difference. In general, we predict a significantly greater reactivity of all mononuclear aqua complexes to biomolecules (average activation barriers of 19−20 kcal/mol) than for both dimers [*cis*-{Pt(NH$_3$)$_2$}(μ-OH)]$_2^{2+}$ (**7a** and **7b**, average barriers 24−26 kcal/mol), demonstrating that {Pt}OH is as a leaving group less efficient than is H$_2$O. The reactivity of [*cis*-{Pt(NH$_3$)$_2$(OH$_2$)}−(μ-OH)−*cis*-{Pt(NH$_3$)$_2$(OH)}]$^{2+}$ (**5**) is smallest (average barrier 28 kcal/mol), which is fully consistent with the high activation barrier for the anation of **5** yielding **4** (Figure 4c).

The activation barrier for Gua platination relative to that of Met platination is a measure of the kinetic selectivity of each complex to guanine versus sulfur-containing biomolecules.[37,38] The calculations reveal that the differences in the selectivity are significant (Figure 4e, Table 1), and the preference for guanine increases in the order: **7a** ≈ **5** < **7b** ≈ **E** ≈ **B** < **C**. Figure 11 displays the calculated transition structures for the reaction of **7a** and **7b** with guanine; additional structures are given in the Supporting Information. The structures and activation barriers indicate that the selectivity to Gua is mainly determined by hydrogen bonding between available hydrogen bond donors in the platinum complex and guanine-O^6, which acts as the hydrogen bond acceptor. The best selectivity to Gua is predicted for *cis*-[Pt(NH$_3$)$_2$(OH$_2$)$_2$]$^{2+}$ (**C**), which mainly arises from a strong stabilization of the transition state for Gua platination by hydrogen bonding involving the aqua ligand.[11] The worst selectivity is predicted for **5** and **7a**. In the TS for the reaction of **5** with Gua, we predict that an ammine ligand is the preferred hydrogen bond donor for Gua, because the aqua ligand is involved in the hydrogen bond to the hydroxo ligand at the other metal center. In the TS for the reaction of **7a** with Gua, a hydroxo ligand is the preferred hydrogen bond donor. There is no aqua ligand in **7a**, elucidating the high activation barrier. This argument is valid for **7b** as well, but this isomer appears to be activated toward the reaction with Gua: In **7b**, the hydrogen of an OH group points already in the direction where guanine-O^6 is located in the transition state.[39]

IV. Pharmaceutical Implications. The computationally predicted quantitative mechanism for the formation, interconversion, and decomposition of dinuclear cisplatin analogues as well as their reactivity and selectivity to biomolecules have important pharmaceutical implications: First, the calculations reveal that the condensation of the mononuclear hydroxo and aqua complexes (**B**−**F**) yielding dinuclear complexes (**1**−**6**) with one bridging hydroxo ligand proceeds via barriers that are lower than those for cisplatin hydrolysis and similar to those for the reactions of mononuclear aqua complexes with biomolecules. At typical micromolar platinum concentrations in tumors, however, only the reaction of *cis*-[Pt(NH$_3$)$_2$(OH$_2$)(OH)]$^+$ (**E**) yielding [*cis*-{Pt(NH$_3$)$_2$(OH$_2$)}−(μ-OH)−*cis*-{Pt(NH$_3$)$_2$(OH)}]$^{2+}$ (**5**) remains kinetically superior to hydrolysis as well as to Gua platination. The experimental fact that in pharmaceutical cisplatin formulations or in blood substitutes diplatinum complexes do not likely form can be explained best by the absence of the highly dimerization-prone species **E** due to suppression of cisplatin hydrolysis (more precisely, due to promotion of

(35) Deubel, D. V. *J. Am. Chem. Soc.* **2004**, *126*, 5999.
(36) Our predicted activation barriers for Gua platination with **B**, **C**, and **E** in aqueous solution show the trend opposite from those reported in another study on the reactions in vacuo at the MP2//HF level: (a) Chval, Z.; Sip, M. *Collect. Czech. Chem. Commun.* **2003**, *63*, 1105. These authors considered reactant adducts rather than the isolated reactants as the reference state, as did others in a study of **C**: (b) Raber, J.; Zhu, C.; Eriksson, L. A. *J. Phys. Chem. B* **2005**, *109*, 11006.
(37) Reedijk, J. *Chem. Rev.* **1999**, *99*, 2499.
(38) It is clear that a slightly lower activation barrier for Gua platination as compared to the barrier for Met platination does not automatically imply that the former reaction is faster, because the pre-exponential factors of the rate constants as well as the concentrations of reactants also affect reaction rates.
(39) H−O−Pt−N(*cis*-ammine) dihedral angle: 69° in **7a**; 87° in **7b**.

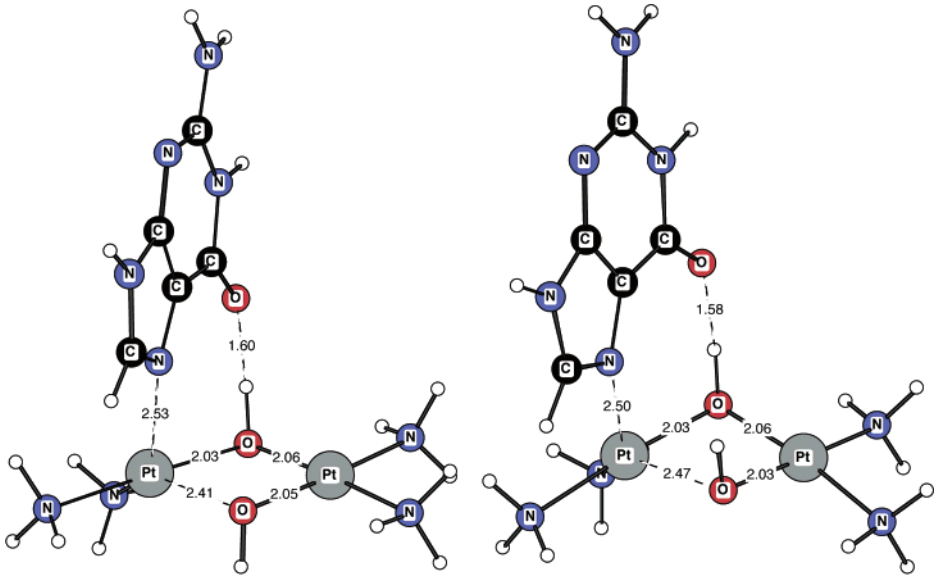

TS **7a** Gua TS **7b** Gua

Figure 11. Calculated transition structures for the reaction of **7a** and **7b** with guanine.

anation) at larger chloride concentrations in these media. Inside the cell nucleus or before the nucleus is reached, the formation of two molecules of **E** requires the hydrolysis of four platinum−chloro bonds of cisplatin, whereas the platination of Gua with mononuclear aqua complexes requires the hydrolysis of only one or two platinum−chloro bonds of cisplatin. Unimolecular cyclization of **5** would have yielded fast the dimer [*cis*-{$Pt(NH_3)_2$}(μ-OH)]$_2^{2+}$, preferentially the propeller-shaped isomer **7a** rather than the butterfly-shaped isomer **7b**. However, if such dinuclear metabolites had formed from cisplatin hydrolysis products at appreciable concentrations inside the cell, their reactions with relevant biomolecules would have been slower than the corresponding reactions of the mononuclear cisplatin hydrolysis products.

Second, the calculated free energy profile in Figure 4 indicates that the toxicity and pharmacological inactivity of di-μ-hydroxo−bis[*cis*-diam(m)ineplatinum(II)] complexes[7] is unlikely due to a greater tendency of these complexes to undergo ligand-substitution reactions with biomolecules, because the predicted activation barriers of the reactions of the dinuclear complexes with Gua and Met are clearly higher than those of the mononuclear complexes. **7a** and **7b** may decompose by successive hydrolysis of both platinum−μ-hydroxo bonds via **5** and TS **EE5**, yielding the mononuclear complex **E** and its conjugated acid **C**. It is possible that **C** or **E** rather than **5**, **7a**, or **7b** react too early with biomolecules before reaching the target cell. Because diplatinum complexes with two μ-hydroxo ligands may decompose to reactive mononuclear complexes, a strategy in the development of new dinuclear complexes can be to avoid this decomposition. The question as to whether di-μ-hydroxo−bis[*cis*-diam(m)ineplatinum(II)] complexes block binding sites of biologically important cations has not been considered in the present work.

Third, several dinuclear Pt(II) anticancer complexes were recently discovered. Our data are not relevant to diplatinum complexes with long flexible α,ω-diaminoalkane linkers,[8,40] but

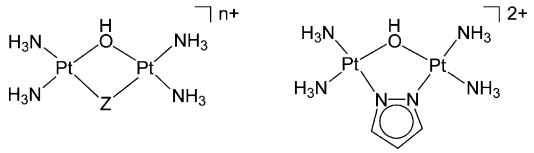

10 **10a**

Figure 12. [*cis*-{$Pt(NH_3)_2$}$_2$(μ-OH)(μ-Z)]$^{n+}$ (**10**) and [*cis*-{$Pt(NH_3)_2$}$_2$(μ-OH)(μ-pyrazolato)]$^{2+}$ (**10a**).

they provide a working hypothesis for the action of new anticancer complexes of the type [*cis*-{$Pt(NH_3)_2$}$_2$(μ-OH)(μ-Z)]$^{n+}$ (**10**, see Figure 12),[6,9] where μ-Z is a bridging ligand, for example, μ-pyrazolato (**10a**), that is more inert than is μ-hydroxo. The calculations imply that the platinum−μ-hydroxo bond in **10** is probably cleaved directly by guanine-N7 rather than via hydrolysis of this bond and subsequent guanine attack: Although the hydrolysis of the μ-hydroxo bond seems relatively facile, [*cis*-{$Pt(NH_3)_2(OH_2)$}−(μ-Z)−*cis*-{$Pt(NH_3)_2$-(OH)}]$^{n+}$ (an analogue of **5**) can be expected to be considerably less reactive to Gua than is **10** (an analogue of **7a**/**7b**). It is clear that **10** does not require the hydrolysis of platinum−chloro bonds as the rate-determining step, which prevents cisplatin from reacting too early with biomolecules. Instead, **10** may avoid such early reactions before reaching the target cell simply because of its smaller reactivity to biomolecules. Based on our data, two reactions appear to be predominant in the mode of action of **10**: (i) The hydrolysis of the μ-hydroxo bond, which may occur already in the bloodstream, but is reversible, leads to a dormant species and has no further consequences. (ii) The other is the relatively slow reaction of **10** with guanine-N7 sites, which is promoted by the high effective concentration of guanine in the cell nucleus.[41] This working hypothesis requires further investigation. Our future work aims to explore how various bridging ligands control the stability of dinuclear complexes and their reactivity and selectivity to biomolecules.

(40) Qu, Y.; Bloemink, M. J.; Reedijk, J.; Hambley, T. W.; Farrell, N. *J. Am. Chem. Soc.* **1996**, *118*, 9307.

(41) Note that the effective guanine concentration in the cell nucleus may be as large as 200 mM, assuming a nuclear volume of 10^{-17} m^3 and up to $\sim 10^9$ available guanine-N7 sites (depending on the position in the cell cycle).

Computational Details

The geometries of molecules and transition states (TS) were optimized at the gradient-corrected DFT level using the three-parameter fit of exchange and correlation functionals of Becke (B3LYP),[15] which includes the correlation functional of Lee, Yang, and Parr (LYP),[16] as implemented in Gaussian 98.[42] The LANL2DZ ECP's[43] and valence-basis sets were used at platinum, and the 6-31G(d,p) basis sets were used at the other atoms.[44] This basis-set combination is denoted II. Vibrational frequencies were also calculated at B3LYP/II. The structures reported are either minima (NIMAG = 0) or transition states (NIMAG = 1) on the potential energy surfaces. Improved total energies were calculated at the B3LYP level using the same ECP and valence-basis set at the metal, but totally uncontracted and augmented with Frenking's set of f functions,[45] together with the 6-311+G(3d) basis sets at sulfur and chlorine and the 6-311+G(d,p) basis sets at the other atoms. This basis-set combination is denoted III+. Activation and reaction free energies (ΔG_a,ΔG_r) were calculated by adding corrections from unscaled zero-point energy (ZPE), thermal energy, work, and entropy evaluated at the B3LYP/II level at 298.15 K, 1 atm to the activation and reaction energies (ΔE_a,ΔE_r), which were calculated at the B3LYP/III+//II level.

Selected molecules have been investigated using a topological analyses of electron density termed "atoms in molecules" (AIM)[30] at the B3LYP/II level; this method was shown to be a useful tool for studying hydrogen bonding.[17g,46] The analysis is based upon those points where the gradient of the density vanishes. In this work, we only consider (3,−1) or bond critical points (BCPs), wherein one curvature (in the internuclear direction) is positive and two (perpendicular to the bond direction) are negative as well as (3,1) or ring critical points (RCPs), wherein one curvature (perpendicular to the ring plane) is negative and two (within the ring plane) are positive. The AIM analysis has been performed using the program package Aimpac.[47] Selected molecules have been investigated at the Becke−Perdew (BP)[48,49] level with a TZV2P basis set at the metal and a TZVP basis set at the other atoms using an energy-decomposition scheme,[32] as implemented in the Amsterdam Density Functional (ADF) package.[50]

Solvation free energies G_{solv}^{ϵ} of the structures optimized at the B3LYP/II level were calculated via Poisson−Boltzmann (PB) calculations with a dielectric constant ϵ of the dielectric continuum that represents the solvent. The PB calculations were performed at the B3LYP level using the LACVP** basis set on platinum and the 6-31G** basis set on the other atoms as implemented in the Jaguar 5 program package.[51] The continuum boundary in the PB calculations was defined by a solvent-accessible molecular surface with a set of atomic radii for H (1.150 Å), C (1.900 Å), N (1.600 Å), O (1.600 Å), S (1.900 Å), Cl (1.974 Å), and Pt (1.377 Å).[52] The calculation of pK_a values with DFT/CDM methods is a challenging task.[53] pK_a predictions were carried out using a thermodynamic cycle,[54] $\Delta G^{\epsilon} = \Delta G^{1} + G_{solv}^{\epsilon}(H^+) + G_{solv}^{\epsilon}(A^-) - G_{solv}^{\epsilon}(A)$ and $pK_a^{\epsilon} = \Delta G^{\epsilon}/RT \ln 10$, where ΔG^1 and ΔG^{ϵ} are the reaction free energies of the reaction, $AH \rightarrow A^- + H^+$, in vacuo and at a dielectric constant $\epsilon = 80.37$ for water, respectively, $G_{solv}^{\epsilon}(X)$ is the solvation free energy of species AH or A^- at ϵ obtained via PB calculations, R is the ideal gas constant, and T is the temperature (298.15 K). Experimental values have been used for the hydration free energy $G_{solv}^{\epsilon}(X)$ of small molecules and ions.[55] A more detailed description of the methods is given in refs 12 and 35.

We believe that continuum dielectric models do not consider properly the changes of solvation entropy in bimolecular reactions; comparisons with experimental values indicate that reactions of platinum complexes and palladium complexes (unpublished) are systematically approximately ∼6 kcal/mol too high. According to Wertz and others,[56] various molecules lose a constant fraction (approximately 0.5) of their entropy, when they are dissolved in water. All free energies in solution except that of the H^+ ion were modified by an entropic term that is one-half (0.5) of the entropy in vacuo with the opposite sign. This empirical correction has led to predicted pK_a values of aqua complexes as well as reaction and activation free energies for the hydrolysis of metal complexes that are in good agreement with experimental values (see the Supporting Information). Using this approach, the predicted activation free energy (15.6 kcal/mol) for the platination of the free guanine molecule with *cis*-$[Pt(NH_3)_2(OH_2)_2]^{2+}$ (**C**) is also in good agreement with the experimental value for guanosine platination (18.3 kcal/mol).[57] The predicted activation free energy (17.9 kcal/mol) for the platination of free guanine with *cis*-$[Pt(NH_3)_2(OH_2)Cl]^+$ (**B**) is 5.5 kcal/mol lower than the experimental activation free energy (23.4 kcal/mol) for the platination of guanine in single-stranded DNA with **B**,[58] which may be attributed partly to the different nature of free guanine and single-stranded DNA. Higher barriers for the platination of guanine in DNA as compared to the platination of free guanine or guanosine may arise from pre-association of cationic complexes with DNA[59] and a subsequent reactivity to its bases according to the Curtin−Hammett principle.[60]

Acknowledgment. This paper is dedicated to Professor Gernot Frenking on the occasion of his 60th birthday. I thank Professor Richard F. W. Bader and co-workers for providing the atoms-in-molecules program package (Aimpac) as well as technical help. This work has been supported by Professor M. Parrinello, the Swiss National Science Foundation, the Fonds der Chemischen Industrie, Germany, the Bundesministerium for Bildung and Forschung, Germany, and the Swiss National Computing Center.

Note Added in Proof. A computational study on the structures of oligonucleotide adducts of **10a** and related complexes appeared recently: Magistrato, A.; Ruggerone, P.; Spiegel, K.; Carloni, P.; Reedijk, J. *J. Phys. Chem. B*, published online Dec. 8, 2005 http://dx.doi.org/10.1021/jp054828p.

(42) Frisch, M. J.; et al. *Gaussian 98*; Gaussian, Inc.: Pittsburgh, PA, 1998.
(43) Hay, P. J.; Wadt, W. R. *J. Chem. Phys.* **1985**, *82*, 299.
(44) (a) Binkley, J. S.; Pople, J. A.; Hehre, W. J. *J. Am. Chem. Soc.* **1980**, *102*, 939. (b) Hehre, W. J.; Ditchfield, R.; Pople, J. A. *J. Chem. Phys.* **1972**, *56*, 2257.
(45) Ehlers, A. W.; Böhme, M.; Dapprich, S.; Gobbi, A.; Höllwarth, A.; Jonas, V.; Köhler, K. F.; Stegmann, R.; Veldkamp, A.; Frenking, G. *Chem. Phys. Lett.* **1993**, *208*, 111.
(46) Gu, J.; Wang, J.; Leszczynski, J. *J. Am. Chem. Soc.* **2004**, *126*, 12651.
(47) http://www.chemistry.mcmaster.ca/aimpac/.
(48) Becke, A. D. *Phys. Rev. A* **1988**, *38*, 3098.
(49) (a) Perdew, J. P. *Phys. Rev. B* **1986**, *33*, 8822. (b) Perdew, J. P. *Phys. Rev. B* **1986**, *34*, 7406.
(50) *ADF 2004.01*; SCM: Amsterdam, The Netherlands; www.scm.com.
(51) *Jaguar 5.0*; Schrodinger, Inc.: Portland, OR, 2000. See: Vacek, G.; Perry, J. K.; Langlois, J.-M. *Chem. Phys. Lett.* **1999**, *310*, 189; www.schrodinger.com.
(52) See: (a) Rashin, A. A.; Honig, B. *J. Phys. Chem.* **1985**, *89*, 5588. (b) Gilbert, T. M.; Hristov, I.; Ziegler, T. *Organometallics* **2001**, *20*, 1183. (c) Baik, M. H.; Friesner, R. A. *J. Phys. Chem. A* **2002**, *106*, 7407. (d) Baik, M. H.; Friesner, R. A.; Lippard, S. J. *J. Am. Chem. Soc.* **2002**, *124*, 4495. We have used a 6-31G+** basis set and a radius of 1.400 Å on the oxygen atoms of aqua and hydroxo ligands.
(53) Jensen, J. H.; Li, H.; Robertson, A. D.; Molina, P. A. *J. Phys. Chem.* **2005**, *109*, 6634.
(54) Jorgensen, W. L.; Briggs, J. M.; Gao, J. *J. Am. Chem. Soc.* **1987**, *109*, 6857.
(55) (a) Barone, V.; Cossi, M. *J. Chem. Phys.* **1997**, *107*, 3210. H_2O, −6.3 kcal/mol; Cl^-, −77.0 kcal/mol. (b) Chambers, C. C.; Hawkins, G. D.; Cramer, C. J.; Truhlar, D. G. *J. Phys. Chem.* **1996**, *100*, 16385. H^+, −260.9 kcal/mol.
(56) (a) Wertz, D. H. *J. Am. Chem. Soc.* **1980**, *102*, 5316. (b) Abraham, M. H. *J. Am. Chem. Soc.* **1981**, *103*, 6742.
(57) Arpalathi, J.; Lippert, B. *Inorg. Chem.* **1990**, *29*, 104. $\Delta H_a = 14$ kcal/mol, $\Delta S_a = -14$ cal/mol K.
(58) Bancroft, D. P.; Lepre, C. A.; Lippard, S. J. *J. Am. Chem. Soc.* **1990**, *112*, 6860. $\Delta H_a = 18$ kcal/mol, $\Delta S_a = -18$ cal/mol K.
(59) Wang, Y.; Farrell, N.; Burgess, J. D. *J. Am. Chem. Soc.* **2001**, *123*, 5576.
(60) Carey, F. A.; Sundberg, R. J. *Advanced Organic Chemistry*; Plenum Press: New York, 2000.

Supporting Information Available: Comparison of experimental and calculated free energies and pK_a values (Table S-1), tabulated values of the energy decomposition of **8** (Table S-2), tabulated relative free energies (Table S-3), separated parts a−e of Figure 4 (Figure S-1), and structural drawings (Figure S-2) of all molecules and transition states given in Figure 4 and of **8**, **9a**, and **9b**. Complete ref 42. This material is available free of charge via the Internet at http://pubs.acs.org.

JA055741K